

Type of the Paper (Original Research)

Occurrence and characterization of Microplastics in the Chili River (Arequipa, Perú) Based on FTIR-ATR and SEM-EDS Analysis

Gerby Giovanna Rondán-Sanabria^{1†}, Holger Saul Perez-Montaña^{1,2}, Edgard Ronny Delgado-Huamani¹ and Italo Francisco Treviño-Zevallos¹

¹Universidad Tecnológica del Perú, Institute of Renewable Energy, Av. Tacna y Arica No. 160, Arequipa 04001, Perú

² Arrhenius Research Institute, Arequipa 04012, Perú

†Corresponding author: Gerby Giovanna Rondán Sanabria; c16238@utp.edu.pe, gerbyrs@gmail.com

<https://orcid.org/0000-0002-8284-7269>: Gerby Giovanna Rondán Sanabria

<https://orcid.org/0000-0002-2406-7862>: Italo Francisco Treviño Zevallos

<https://orcid.org/0000-0001-5615-113X>: Edgard Ronny Delgado Huamani

<https://orcid.org/0000-0001-8997-3009>: Holger Saul Perez Montaña

Key Words	Chili river, Surface water, Microplastics, Plastic waste management
DOI	https://doi.org/10.46488/NEPT.2026.v25i04.D1924 (DOI will be active only after the final publication of the paper)
Citation for the Paper	Rondán-Sanabria, G.G., Perez-Montaña, H.S., Delgado-Huamani, E.R. and Treviño-Zevallos, I.F., 2026. Occurrence and characterization of microplastics in the Chili River (Arequipa, Perú) based on FTIR-ATR and SEM-EDS analysis, <i>Nature Environment and Pollution Technology</i> , 25(4), D1924. https://doi.org/10.46488/NEPT.2026.v25i04.D1924

ABSTRACT

Microplastic contamination in fluvial systems has emerged as a growing environmental concern linked to urban expansion and inadequate plastic waste management. In this study, we assessed the abundance, morphology, color, and polymeric composition of microplastics in the surface waters of the Chili River (Arequipa, Peru). Particles were identified using stereoscopic microscopy and classified according to shape and color, while chemical characterization was performed through FTIR-ATR spectroscopy. Detailed morphological analysis was conducted using scanning electron microscopy coupled with energy-dispersive spectroscopy (SEM-EDS). The analysis revealed a predominance of fibers of various colors (60–80%), followed by foams and fragments. Chromatic distribution varied across sampling sites, with bluish green being the most prevalent color, particularly at TB, where it accounted for 30% of the fibers. FTIR analysis enabled the identification of widely used conventional polymers, including polyethylene (52.4%), polyethylene terephthalate (23.8%), ethylene-vinyl acetate, and polyurethane. SEM micrographs exhibited irregular surfaces, cracks, delamination, and cavities, consistent with progressive physical degradation. EDS analysis was also used as a complementary tool to evaluate elemental surface features and possible inorganic

deposits, while polymeric identification was based primarily on FTIR-ATR results. These findings suggest that the microplastics present in the Chili River are compatible with environmental aging and secondary fragmentation processes, reflecting the influence of urban activities on fluvial contamination dynamics.

1. INTRODUCTION

Since the mid-twentieth century, plastics production has surged to exponential levels, posing a global threat that impacts almost every ecosystem globally (Yang et al. 2024). Projections indicate that more than 700 million tons of plastic waste could accumulate in aquatic and terrestrial environments by 2040 (Lau et al. 2020). This increase, driven by unsustainable consumption patterns and deficiencies in waste management systems, has positioned plastic pollution as one of the most pressing emerging environmental challenges worldwide (Barnes et al. 2009; Peng et al. 2018). Due to their persistence and slow degradation rates, polymers such as polypropylene (PP), polycarbonate (PC), and polyvinyl chloride (PVC) can remain in the environment for extended periods, progressively fragmenting into particles smaller than 5 mm, known as microplastics (MPs) (Österlund et al. 2023).

Rivers serve as fundamental transport pathways for microplastics from terrestrial sources to the oceans, functioning both as conduits and temporary reservoirs (Yang et al. 2024; Joshi et al. 2025). It is estimated that countries with high levels of mismanaged plastic waste may contribute substantially to riverine plastic discharge into marine environments (Upadhyay and Bajpai, 2021; Belli et al. 2026). Additionally, recent studies have demonstrated that microplastics represent not only a physical contaminant but also a relevant fraction of fossil-derived particulate organic carbon in fluvial systems, potentially altering biogeochemical processes and the global carbon cycle. For example, in large-scale systems such as the Yellow River, annual transport has been estimated at up to 7.73×10^{16} particles delivered to the ocean, underscoring the magnitude of the problem at the watershed scale (Liu et al. 2025).

Numerous investigations have documented the widespread presence of microplastics in river systems with varying degrees of urbanization and anthropogenic pressure. Studies conducted in tropical rivers in Malaysia have shown that MP abundance and composition are strongly influenced by urban activities, wastewater discharge, and hydrodynamic conditions (Anuar et al. 2023). In Asian river systems (Xiang et al. 2026), population density, industrialization, and regional climatic variability have been identified as key drivers influencing the spatial distribution and ecological risk of microplastics. Likewise, the Jamuna River in India reported high concentrations of fibers and fragments, with polymers such as PE, PET, and PP predominating, along with moderate to high ecological risk indices (Islam et al. 2025). In the Latin American context, recent assessments in Brazilian rivers highlight the predominance of fibers and common polymers such as PE and PP, while emphasizing the need for more comprehensive regional studies (Lebreton and Andrady, 2019; Belli et al. 2026). In this sense, the Amazon basin has been identified as a critical region in the transfer of plastics to the Atlantic Ocean, with

the Amazon River recognized as one of the main global contributors (Giarrizzo et al. 2019; dos Santos Silva et al. 2024).

Recent research in high-Andean systems of southern Peru has also reported significant microplastic concentrations in strategic freshwater reservoirs, such as the Colca–Chili system in Arequipa. These studies indicate that climatic factors such as wind dynamics, precipitation, and solar radiation play a crucial role in particle transport, fragmentation, and degradation, favoring the accumulation of fibers and particles smaller than 1 mm (Banda et al. 2025). In the Arequipa context, the Quilca–Vitor–Chili watershed has shown a predominance of fibers and polymers such as PE and PP associated with urban sources and the weathering of larger plastic debris, which contributes to the generation of secondary microplastics (Larrea Valdivia et al. 2025). Therefore, the present study aims to characterize the shape, color, and polymeric composition of microplastics in the surface waters of the Chili River using stereoscopic microscopy, FTIR-ATR, and SEM-EDS, and interpret their degree of environmental transformation through the integration of chemical and morphological evidence. Within this context, this research seeks to advance understanding of microplastic behavior in urban fluvial systems of the Andean region and to provide scientifically robust information for evaluating their environmental impact.

2. MATERIALS AND METHODS

2.1. Reagents and equipment

The materials used in this study were made of glass or stainless steel to prevent contamination from plastic residues. Likewise, all reagents were of analytical grade and purchased from Sigma-Aldrich. Infrared spectroscopic analyses were conducted using a Bruker FTIR-ATR system (Model 3120), while morphological identification was performed with a LABTRON stereomicroscope (Model LSM-B12). High-resolution imaging and elemental characterization were carried out using a Thermo Scientific (Model Scios 2) scanning electron microscope equipped with energy-dispersive spectroscopy (SEM-EDS).

2.2. Study area

Arequipa is the second most populous city in Perú, located on the western slope of the Andes at an altitude of approximately 2,320 m above sea level. Based on data from the National Institute of Statistics and Informatics (INEI), the metropolitan area of Arequipa has an estimated population ranging between 1.1 and 1.2 million inhabitants. Several industrial facilities operate both within and around the city, some of which are situated along the banks of the Chili River. The Chili River forms part of the Quilca–Vitor–Chili watershed system, which covers an area of 13,529 km². Its river network flows predominantly from east to west before discharging into the Pacific Ocean (Carpio Fernández et al. 2022).

In this study, four sampling sites were selected along an approximately 8 km urban stretch of the river, identified as Chilina (CH), Av. La Marina (AM), Tingo (TI), and Tiabaya (TB) (Fig. 1). Sampling was conducted during three periods: May (after the rainy season, which extends from December to March) and subse-

quently in July and September. The initial sampling campaign followed a period of intense rainfall that generated extreme turbidity and significant sediment transport, conditions that hindered microplastic identification. These points were selected due to their accessibility and because they include areas of tourist, recreational, and agricultural relevance.

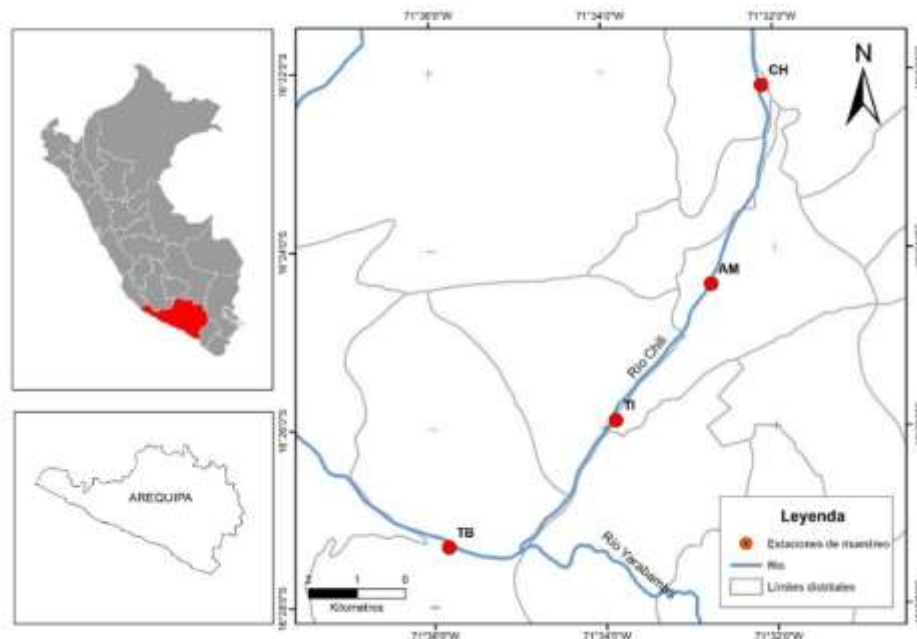


Fig. 1: Sampling sites on the Chili River in the city of Arequipa

2.3. Sampling of water

Surface water from the river was collected from the designated sites (Fig. 1). No plastic materials were used during sampling to prevent contamination. At this stage, river water was collected using a 10 L stainless steel bucket with a lid, which was immersed to a depth of approximately 5 cm against the current. The collected water was transported to the laboratory in sealed 4 L glass bottles and collected in triplicate at each sampling point. Every material used throughout the procedure was thoroughly rinsed with distilled water prior to use to minimize potential contamination.

2.4. Sampling preparation

First, the material retained on the sieve was transferred to a glass beaker for subsequent treatment with potassium hydroxide. In parallel, 1 L of water was measured and filtered through a 200 μm mesh, followed by organic matter digestion (Mahmud, Roy, Md. Mahmud Kamal Bhuiyan, et al. 2025), with minor modifications. For this purpose, 10% potassium hydroxide (KOH) was added at a ratio of 2:1 (solution to sample) for organic digestion and kept at 50 $^{\circ}\text{C}$ for 24 h. Following digestion of the organic content, density separation was performed using a saturated sodium chloride (NaCl) solution ($\sim 1.2 \text{ g/cm}^3$), facilitating the flotation of microplastics. The $\geq 200 \mu\text{m}$ fraction corresponded to particles initially retained by the mesh, whereas the $\geq 8 \mu\text{m}$ fraction

corresponded to particles subsequently recovered through vacuum filtration. Both stages were part of the same sequential procedure applied to the same processed sample.

Supernatant was carefully recovered and subjected to vacuum filtration using Whatman No. 4 filter paper, with an approximate retention size of 8 μm . All procedures were conducted in triplicate to verify recovery efficiency, employing analytical-grade reagents and ultrapure water. Finally, the filter papers were placed in glass Petri dishes, covered with aluminum foil, and preserved for subsequent microscopic analysis.

Although procedural blanks and specific airborne contamination controls were not performed, glass and stainless-steel materials were used throughout all analytical stages, and the samples were kept covered with aluminum foil to minimize external contamination. Therefore, the predominance of fibers observed in this study should be interpreted with caution, considering the potential influence of environmental contamination inherent to microplastic processing.

2.5. Microplastics Separation

Once the MPs were extracted, the retained particles on the filter paper were examined under a stereomicroscope and manually sorted using ultra-fine forceps based on their shape and color. Although gravimetric quantification of the recovered particles would have provided additional information, this approach was not feasible due to the extremely small size of the MPs.

Despite this limitation, the particles were successfully isolated and categorized for subsequent polymer identification using FTIR-ATR analysis. Selected MPs were also mounted onto double-sided carbon adhesive tape to enable detailed surface and morphological characterization by scanning electron microscopy coupled with energy-dispersive spectroscopy (SEM-EDS). Sample preparation required microscopic assistance to ensure precise manipulation and positioning of individual particles.

2.6. Chemical characterization by FTIR-ATR

Polymers were identified, and functional group analysis of the isolated MPs was conducted using a Bruker Model 3120 Fourier Transform Infrared (FTIR) spectrometer equipped with a diamond attenuated total reflectance (ATR) accessory. Spectral measurements were acquired over a range of 4000–400 cm^{-1} , using 24 scans per sample at a resolution of 4 cm^{-1} . All analyses were performed in triplicate to ensure reproducibility. These spectra were normalized at 3760 cm^{-1} , a region where the baseline remained stable, and interference from atmospheric water vapor was minimal. This normalization was necessary because absolute absorbance intensity depends on the extent of contact between the sample and the ATR crystal surface, a parameter that cannot be precisely controlled during measurement.

2.7. Scanning Electron Microscopy (SEM) and Energy-Dispersive Spectroscopy (EDS)

The surface morphology of the microplastics was examined using scanning electron microscopy (SEM) equipped with an Everhart–Thornley detector (ETD), operating at a working distance of 7–12 mm. Elemental composition analysis was carried out by energy-dispersive X-ray spectroscopy (EDS). A Thermo Scientific Scios 2 microscope was employed to evaluate the morphological features of the MPs, using magnifications

ranging from $125\times$ to $10,000\times$. To prevent charge accumulation during analysis, the samples were previously coated with a thin gold layer using a Q150R ES Plus sputter coater (Quorum Technologies) for 2 minutes prior to imaging.

2.8. Data Analysis

The results obtained were processed using Origin Pro 2025 software. Data are reported as mean values \pm standard deviation (SD). Standard deviation was calculated to assess variability among sampling sites and particle categories. Given the exploratory nature of the study and the limited number of samples per site, inferential statistical tests were not applied. Accordingly, the analysis focuses on descriptive statistics to highlight distribution patterns in particle shape, color, and polymer type.

3. RESULTS AND DISCUSSIONS

3.1. Abundance and distribution of microplastics

The surface water samples at the different sampling sites showed no visible debris and were characterized by a transparent appearance. However, given that microplastics (MPs) are not detectable to the naked eye, all samples were filtered using a $200\ \mu\text{m}$ mesh to recover larger microplastic particles as well as associated organic residues. Results are shown in Table 1 and report the mean abundance of MPs in the surface waters of the Chili River across the four sampling sites during three seasons (autumn, winter, and spring). For the estimation of abundance, two size fractions ($\geq 200\ \mu\text{m}$ and $\geq 8\ \mu\text{m}$) were considered to obtain a comprehensive approximation of the total number of microplastics per liter of water. The findings indicate that MPs were present in all seasons and at all sampling sites, suggesting widespread contamination along the studied river stretch, both spatially and temporally. Clear differences were observed among sites and seasons. A descriptive pattern of increasing microplastics abundance from CH to TB was observed across the sampling periods (Table 1), suggesting cumulative influence of urban activities along the studied rivers section.

This spatial pattern may be associated with the influence of downstream urban activities and aligns with findings reported for the Quilca–Vitor–Chili watershed, where a generalized presence of MPs in surface waters was documented, along with higher abundances associated with urban and agricultural pressures in publicly accessible sites (Larrea Valdivia et al. 2025). A similar trend was reported by (Kunz et al. 2023). In the Jamuna River (Bangladesh), where river sections flowing through densely populated areas exhibited significantly higher MP concentrations than less urbanized stretches, a pattern attributed to domestic effluents and urban waste inputs. In contrast, the seasonal increase in microplastic abundance may be interpreted as a response of the fluvial system to post-rainfall redistribution processes, peaking during spring. In this season, the highest abundance was recorded at site TB, with 23.00 ± 2.00 and 128.33 ± 4.02 MPs/L, whereas the lowest values were observed at CH, with 11.33 ± 1.53 and 32.33 ± 2.52 MPs/L (Table 1).

During the rainy season (summer, December to March), however, MPs may become dispersed, diluted, or deposited in sediments and along riverbanks, thereby reducing their detectability within the water column. In contrast, during the dry and transitional periods (autumn to spring), characterized by elevated solar radiation

and higher temperatures, plastic debris exposed along the banks of the Chili River may undergo photo-oxidation and secondary fragmentation. These processes likely contribute to the generation of smaller microplastic particles and their gradual release into the river channel, which may explain the increased abundance observed during spring. This behavior was observed in the Ariyankuppam River (India), where surface-water MP concentrations do not reach their highest levels during periods of intense rainfall, but rather during subsequent stages when discharge decreases and previously deposited materials are remobilized (Joshi et al. 2025). In the same way, in fluvial sediments of the Qin River (China), surface sediment layers were found to accumulate MPs particularly fibers and small fragments which may be resuspended into the river channel under variable hydrodynamic conditions (Ma et al. 2025). Similarly, the same behavior was reported in Asian rivers, where reduced discharge promotes the release of microplastics stored in sediments, thereby increasing concentrations in the water column (Yang et al. 2025).

Moreover, integrating the 200 μm and 8 μm size fractions enabled the capture of a substantial proportion of fine microplastics, contributing to a more representative estimate of actual MP abundance per liter of water at the time of sampling (Fig. 2). An apparent increase in MP concentrations from Chilina (CH) to Tiabaya (TB), primarily driven by fibers. In addition, recent methodological studies caution that the inclusion of smaller size fractions may substantially elevate reported abundance values and complicate direct comparisons across studies. Nevertheless, this approach provides a more comprehensive assessment of the true magnitude of microplastic contamination in fluvial systems (Büngener et al. 2024; Venkatachalam and Radhakrishnan, 2025).

In general, the findings for the Chili River are consistent with evidence reported for urban rivers worldwide. The observed patterns suggest that this river stretch may be influenced by anthropogenic activities, including informal dumping sites, solid waste discharge, restaurants, hotels, and densely urbanized areas, all of which contribute significantly to microplastic contamination along this section of the river.

Table 1. Abundance of microplastics identified per liter of water sampled in May, July, and September

Sampling Site	Season					
	May/Autumn		July/Winter		September/Spring	
	$\geq 200 \mu\text{m}$	$\geq 8 \mu\text{m}$	$\geq 200 \mu\text{m}$	$\geq 8 \mu\text{m}$	$\geq 200 \mu\text{m}$	$\geq 8 \mu\text{m}$
CH	2.33 \pm 0.58	5.33 \pm 1.53	7.00 \pm 1.00	17.67 \pm 2.08	11.33 \pm 1.53	32.33 \pm 2.52
AM	4.00 \pm 1.00	13.00 \pm 2.00	11.33 \pm 0.58	48.00 \pm 2.00	16.33 \pm 1.43	81.33 \pm 2.31
TI	6.00 \pm 1.00	18.33 \pm 1.53	14.00 \pm 1.00	59.67 \pm 2.52	20.33 \pm 1.00	95.00 \pm 5.00
TB	6.67 \pm 1.53	19.33 \pm 2.08	16.67 \pm 1.53	62.00 \pm 2.00	23.00 \pm 2.00	128.33 \pm 4.02

CH: Chilina, AM: Avenida la Marina, TI: Tingo, TB: Tiabaya

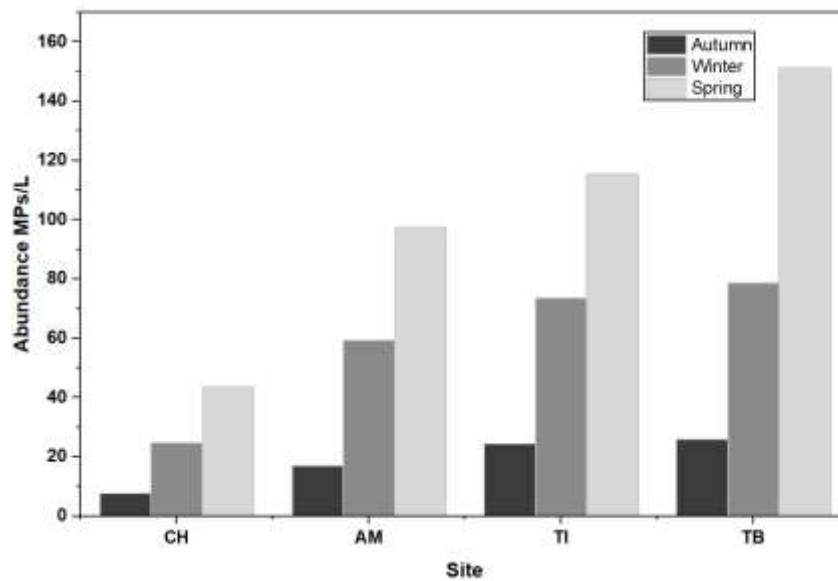


Fig. 2. Total abundance of microplastics by season and water sampling site in the Chili River

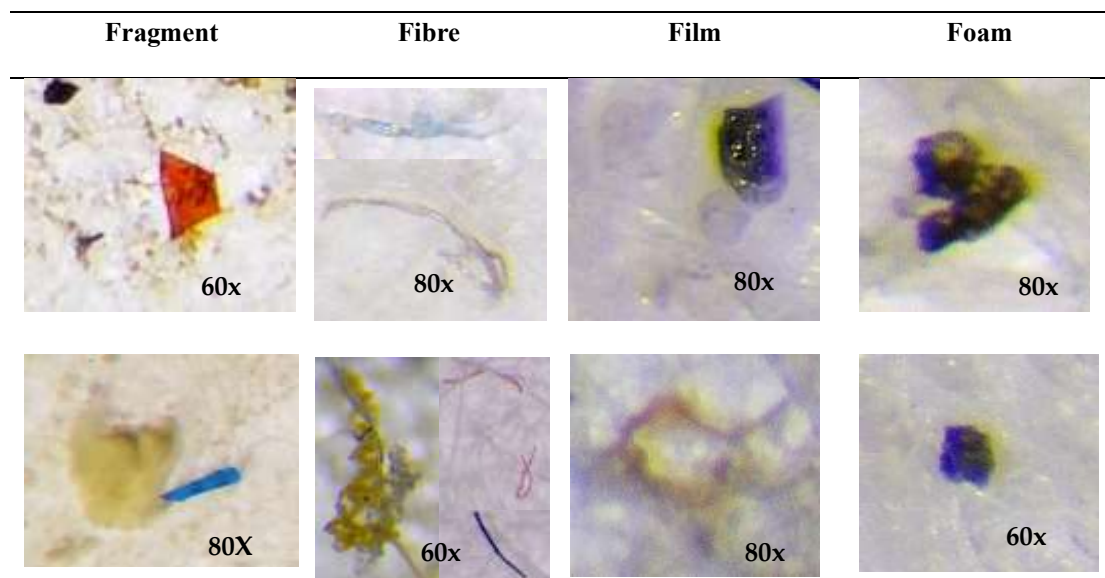
3.2. Types of plastics, shape and color

Fig. 3 shows the morphological forms of MPs identified through stereoscopic microscopy at magnifications of 60 \times and 80 \times . Four primary microplastic morphotypes were distinguished: fragments, films, fibers, and foams-based on their color, morphology, and surface appearance under microscopic observation. The particles extracted from the filters corresponded predominantly to blue-green, pink, and purple fibers, indicating a significant contribution from anthropogenic sources, particularly synthetic textiles and commonly used plastic materials. The larger fibers, fragments, films, and foams were selected and grouped for subsequent characterization by FTIR-ATR. However, some smaller MPs could not be manually retrieved using forceps due to their reduced dimensions and, consequently, were not subjected to spectroscopic analysis. This methodological limitation has been reported in similar studies and is associated with the inherent challenges of handling micrometric-scale MPs (Hidalgo-Ruz et al. 2012; Gune and Martin, 2025).

Fig. 4 presents the percentage distribution of MPs by shape, color, and polymer type in the Chili River. Among the identified particles, fibers were the dominant form, representing 60% at site CH (46 fibers) and 80% at TB (195 fibers) (Fig. 4A). Foams constituted the second most abundant category, with 15 units at CH, accounting for 20% of the total at that site. Films were observed in intermediate proportions, ranging from 5 to 15% across sampling sites, whereas fragments were identified at comparatively lower percentages. These patterns are consistent with those documented in other fluvial systems, where fibers typically constitute the most abundant fraction of MPs (Anuar et al. 2023; Harini et al. 2025; Khan et al. 2025a; Ullah et al. 2025). Similarly, the present findings align with reports from the Quilca Vitor Chili (Larrea Valdivia et al. 2025), indicating a predominant contribution from domestic discharges, synthetic textile fibers, and solid waste deposited along riverbanks.

Concerning the distribution of color (Fig. 4B), bluish-green particles exhibited the highest percentages, with similar values ranging from 25–30% at CH, AM, and TI, and approximately 30% at TB. These were followed by pink (10–20%) and transparent particles (10–15%). Red particles showed intermediate proportions (5–12%), whereas black-gray particles remained below 10% at all sampling sites. The predominance of bright and visibly colored particles may reflect the contribution of secondary plastics derived from packaging materials, household utensils, and dyed synthetic fibers. Additionally, variations in particle color may also be associated with environmental weathering processes, including pigment fading, bleaching, and photo-oxidative degradation during prolonged exposure to sunlight and environmental conditions, which can alter the original coloration of plastic materials (Deocarís et al. 2023). Comparable patterns have been reported in other fluvial systems, though with considerable regional variability. For example, in the Buriganga and Turag rivers, white particles and colors such as red and black were dominant (Mahmud, Roy, Md Mahmud Kamal Bhuiyan, et al. 2025) whereas in the Pearl River Delta, white (36%) and transparent (20.2%) particles prevailed (He et al. 2025).

The same way, in highly urbanized systems such as the Diep River, black-gray particles accounted for up to 47% of the total MPs (Khan et al. 2025b), a distribution directly associated with tire wear and traffic-related particles, consistent with findings for heavily trafficked urban watersheds (Österlund et al. 2023). However, in the Chili River, the relatively low proportion of black particles and the predominance of colored fibers suggest that domestic discharges and urban solid waste represent the principal sources, rather than intense road runoff. Overall, the integration of shape, color, and polymer composition revealed the predominance of polyethylene (PE, 52.4%), followed by polyethylene terephthalate (PET, 23.8%), ethylene vinyl acetate (EVA, 19.0%), and polyurethane (PUR, 4.8%) (Fig. 4C), among the FTIR – confirmed particles.



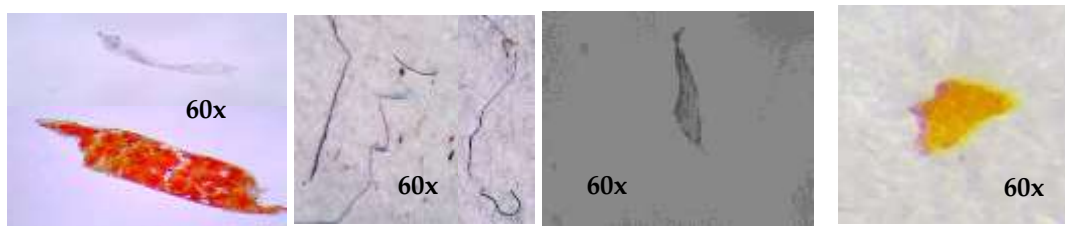


Fig. 3. Representative stereomicroscope images of the distinct microplastics forms detected in surface waters of the Chili River

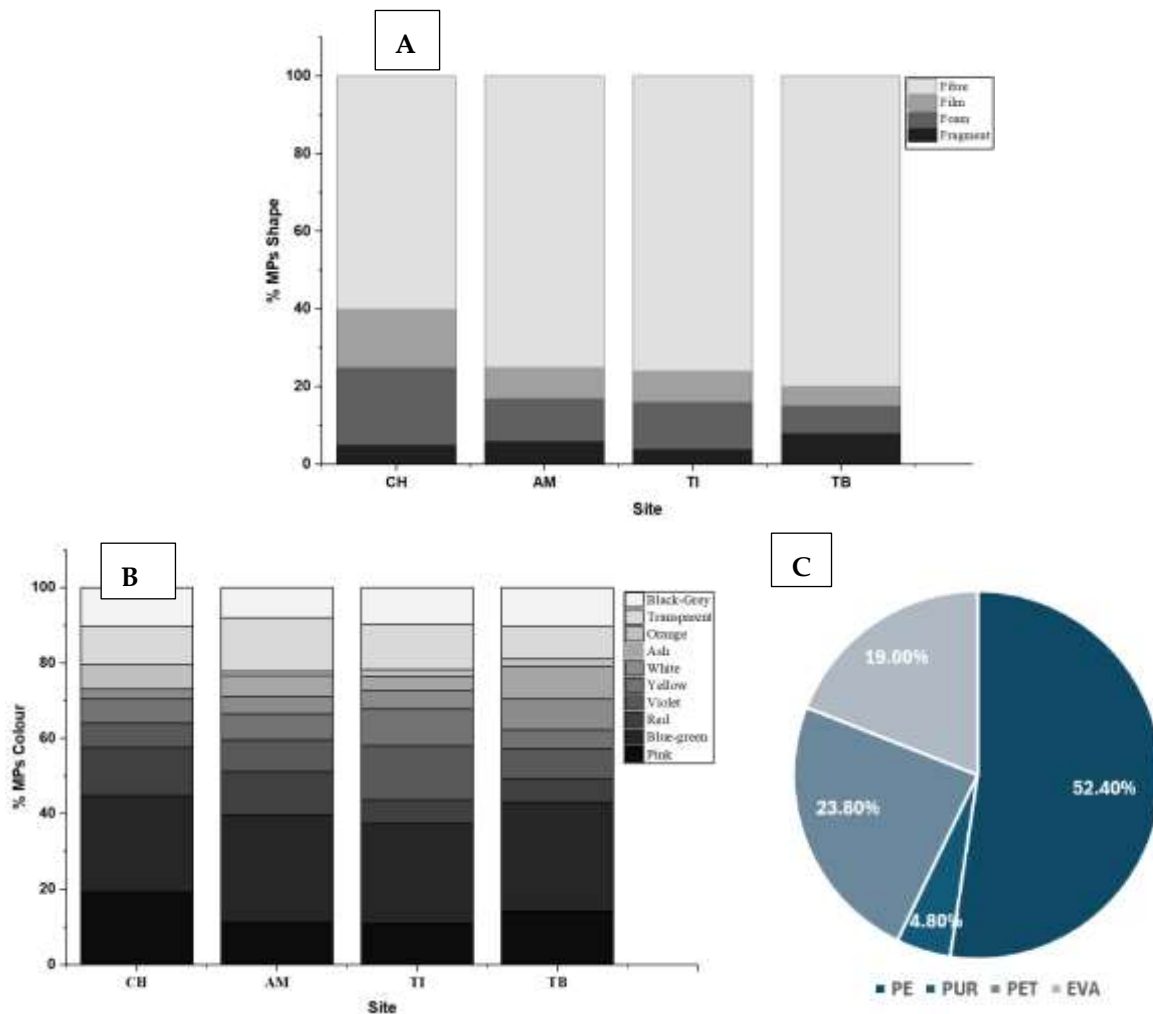


Fig. 4: (A) Percentage distribution of microplastic forms; (B) color distribution of MPs; and (C) relative abundance of polymers identified by FTIR-ATR

3.3. Chemical characterization of polymers

Before the spectroscopic analysis, selected microplastic (MP) particles were individually isolated and enumerated for FTIR characterization. A total of 34 visually identified particles and one additional particle labeled as P Mic were subjected to FTIR-ATR analysis. However, only 21 particles generated spectra with sufficient quality for reliable chemical identification. The remaining particles could not be conclusively identified due to

their extremely small size, limitations associated with the absence of a micro-FTIR system, or insufficient spectral matching with the reference library. Therefore, the polymer percentages reported in this study correspond only to FTIR-confirmed particles and should not be interpreted as representative of all visually identified particles.

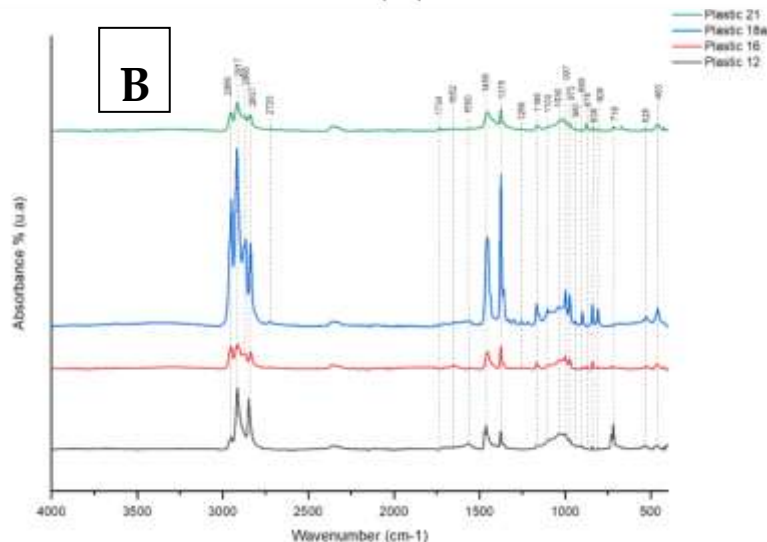
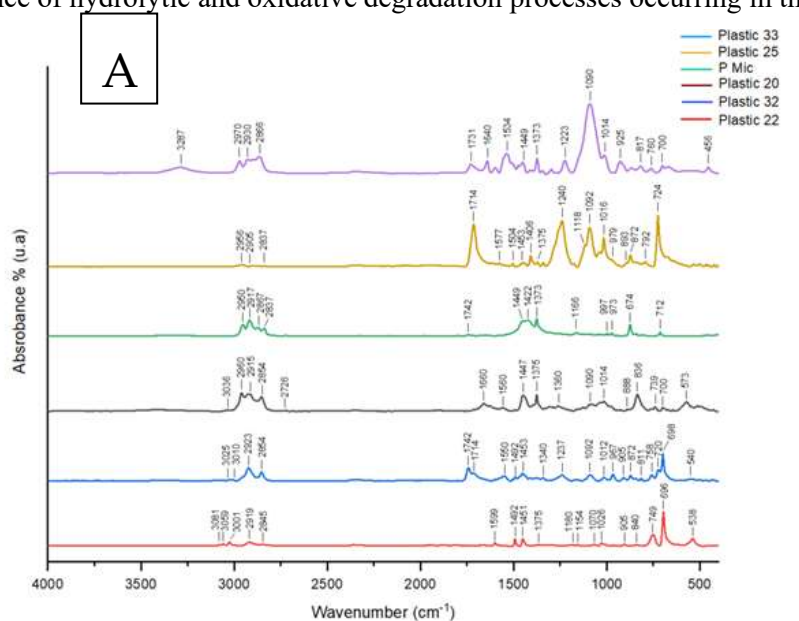
The FTIR spectra of plastic macro-samples collected along the shore of the Chili River in Arequipa, Peru revealed distinct functional groups that allowed classification into three spectrally defined groups (Fig. 5): spectra showing evidence of advanced environmental degradation, including O-H or N-H vibration and/or emergence of new carbonyl, aldehydic, and associated bands linked to hydrolysis and photo-oxidation (Norrish I and II) (Fig. 5A), spectra without clear O-H/N-H signatures of hydrolysis but with relatively complex fingerprint regions characteristic of intact or moderately aged engineering polymers (Fig. 5B), and spectra dominated by CH stretching and simple fingerprint patterns indicative of hydrocarbon-rich polymers with limited heteroatom functionality (Fig. 5C). Across all samples, characteristic absorption bands were consistently detected at 3200–3500 cm^{-1} (broad O-H/N-H stretching region), 2500–3100 cm^{-1} (CH stretching of methylene and methyl groups), and 1600–1800 cm^{-1} (carbonyl stretching), with additional features between 1600–1000 cm^{-1} corresponding to O=C=O, C–C, C–O–C, and C–C–O vibrations; weak interactions were noted at 1040 cm^{-1} (C–N) and 800–400 cm^{-1} (C–O and CH₂ bending), while polymer backbone linkages were suggested by C–C–C stretching near 1100 cm^{-1} .

In Fig. 5A, samples Mic, 32, 22, and 20 exhibited O-H stretching band at $\sim 3294 \text{ cm}^{-1}$ and H–O–H bending at 1648 cm^{-1} , which may indicate hydrolytic processes or the presence adsorbed moisture (Kotov, Keskitalo and Johnson, 2025). A distinct CHO band at 2722–2726 cm^{-1} is compatible with oxidative chain scission and may be with polyethylene glycol and ethylene vinyl acetate (EVA) systems (Demri et al. 1994; Allen et al. 2000). Carbonyl stretching (1740–1731 cm^{-1}) and ester-related bands (1160 cm^{-1}) confirmed early degradation stages (Allen et al. 2000; Jin, Chen and Zhang, 2010), with additional CH₂ and CH₃ vibrations (2917, 2867, 1375 cm^{-1}) and vinyl CH out-of-plane bending (995, 960, 840 cm^{-1}) supporting EVA identification (Rozenberg, Loewenschuss and Marcus, 1998; Allen et al. 2000). Sample 33 showed NH stretching (3287 cm^{-1}) and N–H bending (1534 cm^{-1}) (Coleman et al. 2002; Skrovanek, Painter and Coleman, 2002), alongside urethane carbonyl (1731 cm^{-1}) and urea carbonyl (1640 cm^{-1}) in polyether systems (Wang and Cooper, 2002), confirming polyurethane (PUR) presence; strong C–O stretching (≈ 1090 and 1223 cm^{-1}) further indicated possible urethane network rearrangements or oxidative modification (De Zea Bermudez, Carlos and Alcácer, 1999; Mishra et al. 2006; Valdés et al. 2018). Sample 25 displayed CH₃ and CH₂ stretching (2956 and 2837 cm^{-1}) (Chen, Hay and Jenkins, 2012; Tariq et al. 2020). Furthermore, five diagnostic peaks (1714, 1240, 1090, 872, 724 cm^{-1}) corresponding to ketones (C=O), aromatic/aliphatic ethers (C–O), and aromatic C–H bonds, consistent with polyethylene terephthalate (PET) (Chen, Hay and Jenkins, 2012; Ioakeimidis et al. 2016; Dodi et al. 2022; Dimassi et al. 2023).

In Fig. 5B, spectra lacked OH/NH vibrations; Samples 21, 18, 16, and 12 exhibited CH₃/CH₂ stretching (2956, 2917, 2866, 2837 cm^{-1}) (Tariq et al. 2020; Dimassi et al. 2023). Aging degradations are suggested by the initial presence of carbonyl (C=O) groups at $\sim 1740 \text{ cm}^{-1}$, indicating oxidative modification rather than ester

formation. Shifts in bands at 1652 and 1560 cm^{-1} may reflect secondary oxidation products or conjugated structures formed during photo-oxidative aging. Norrish II contributes to the formation of carbonyl and vinyl groups via chain scission (Phan, Padilla-Gamiño and Luscombe, 2022). Samples exposed to deionized water show peaks at 1100 cm^{-1} and, especially, at 1000 cm^{-1} ; these bands are consistent with C-O stretching and vinyl related vibrations associated with polypropylene oxidation rather than exclusively indicating a Norris type II reaction (Gewert, Plassmann and Macleod, 2015; Fernández-González et al. 2021; Phan, Padilla-Gamiño and Luscombe, 2022). The characteristic polypropylene peaks (1460, 1376, 1167, 997, 973 cm^{-1}) confirm polypropylene composition (Oreski and Wallner, 2009; Glaser et al. 2019; Tariq et al. 2020). Overall, the coexistence of carbonyl formation and diagnostics polypropylene bands indicate photo-oxidative aging with chain scission processes rather than predominant crosslinking recombination products.

In Fig. 5C, spectra of samples 29, 28, 27, 10, 5, 24, 14, 11, 4, 2, and 1 showed simpler functional group patterns dominated by CH stretching and limited fingerprint complexity, with diagnostic peaks at 2915, 2848, 1463, and 718 cm^{-1} assigned to CH_2 asymmetric stretching, CH_2 symmetric stretching, bending deformation, and rocking deformation, respectively, consistent with polyethylene (PE) (Chiu and Hsiao, 2005; Glaser et al. 2019; Maheswaran et al. 2022; Xu et al. 2024; Khan et al. 2025c). Overall, the FTIR results demonstrate the presence of EVA, polyurethane, PET, polypropylene, and polyethylene among the collected plastics, with clear evidence of hydrolytic and oxidative degradation processes occurring in the Chili River.



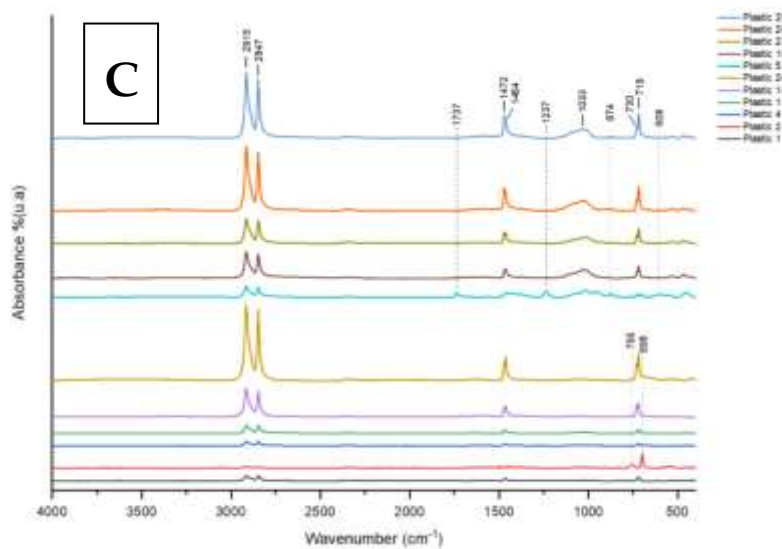


Fig. 5: FTIR spectra of the different microplastics identified in the surface waters of the Chili River: (A) EVA, PUR, and PET, (B) PP: and (C) PE

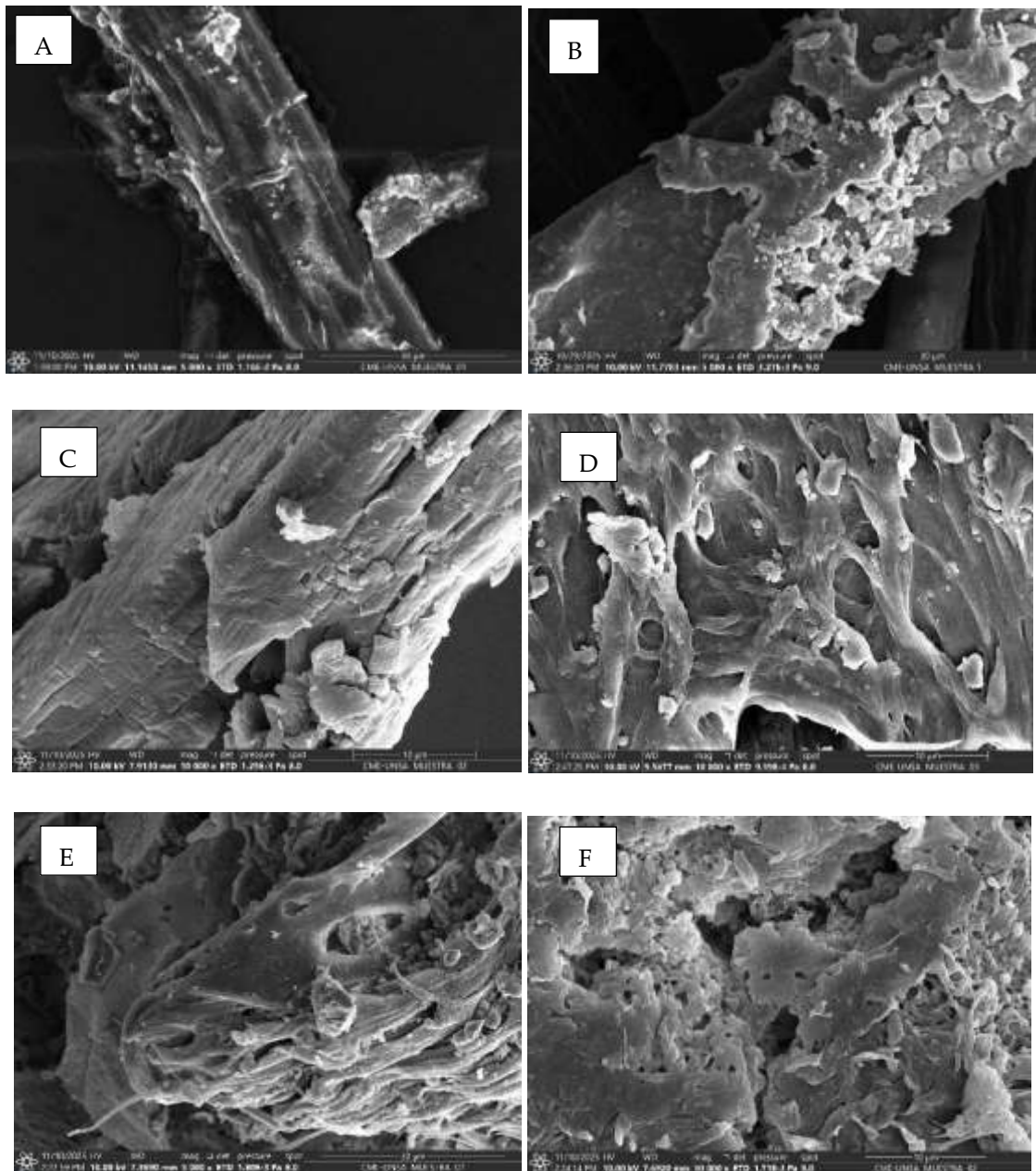
3.4. Morphological Characteristics of Microplastics in Water

Fig. 6 presents the morphological features of microplastics obtained by scanning electron microscopy (SEM). The micrographs (Fig. 6A–H) reveal polymer surfaces exhibiting varying degrees of environmental degradation. Fig. 6A–B shows a fibrous morphology with an irregular surface and adhered material accumulation can be observed, whereas in other particles (Fig. 6C–H), cracks, delamination, cavities, and brittle fractures predominate. These characteristics are consistent with combined processes of mechanical abrasion, oxidative photodegradation, and physical erosion, as described in fluvial systems where SEM analyses frequently reveal rough surfaces, edge cracks, and irregular topography as consequences of environmental aging (Alam, Shammi and Tareq, 2023),(Mahmud, Roy, Md. Mahmud Kamal Bhuiyan, et al. 2025; Ullah et al. 2025; Venkatachalam and Radhakrishnan, 2025). Likewise, studies conducted in Southeast Asian rivers report surface fissures and structural cohesion loss associated with progressive oxidation and secondary fragmentation (Anuar et al. 2023).

SEM-EDS analysis was used as a complementary method to evaluate elemental surface features and possible inorganic deposits on the particles. Even though carbon and oxygen were commonly detected, these signals were not interpreted as independent confirmation of polymer identity, especially considering the gold coating applied before SEM analysis and the possible presence of environmental mineral or salt deposits. The occasional detection of Na, Cl, or K was therefore interpreted as evidence of superficial deposits rather than as part of the polymer structure. Polymer identification was based primarily on FTIR-ATR analysis.

The observed morphological alterations are also comparable to reports in which SEM has been used to interpret the degree of weathering and transport potential, often associated with increased surface grooves,

scratches, and rounded edges (Venkatachalam and Radhakrishnan, 2025). In that context, the presence of rough surfaces and linear fractures in particles from the Chili River may reflect prolonged environmental exposure and progressive degradation. This evidence is consistent with the FTIR results (Fig. 5A–C), where EVA, PUR, PET, PP, and PE exhibited oxidation-related signals and structural modifications, suggesting an ongoing environmental weathering process in the Chili River. Overall, the combined SEM, EDS, and FTIR observations are consistent with environmental weathering and aging processes affecting the analyzed particles within the fluvial system.



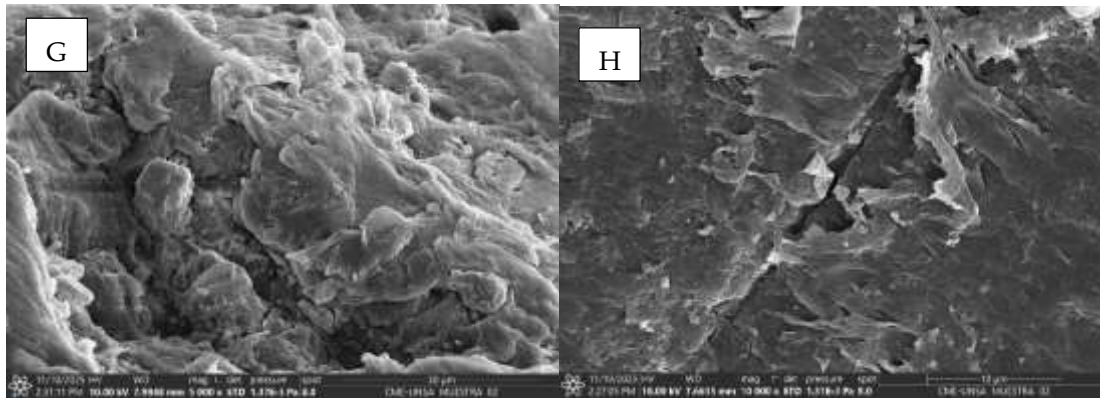


Fig. 6: Scanning electronic microscopy (SEM) images: (A-B) Fibers; (C-D) Fragments, (E-F) Foam, (G-H) Film

4. CONCLUSIONS

The present study reveals the widespread presence of microplastics in the surface waters of the Chili River, highlighting the influence of anthropogenic activities on the generation, transport, and transformation of fluvial pollution. The predominance of fibers and fragments, together with the identification of conventional polymers such as PE, PP, PET, EVA, and PUR through FTIR-ATR analysis, reflects the contribution of commonly used plastic materials and their subsequent environmental fragmentation. The integration of spectroscopic and microscopic analyses enabled the identification of environmental transformation signals, including the formation of carbonyl groups and modifications in characteristic absorption bands, as well as surface features such as cracks, delamination, and cavities observed by SEM. This evidence is consistent with environmental weathering and secondary fragmentation processes affecting the analyzed particles.

Taken together, the results emphasize the importance of applying integrated approaches that combine morphological and chemical characterization to better understand the environmental behavior of microplastics in Andean fluvial systems. The information generated provides a relevant scientific foundation for future risk assessments and for the development of management and mitigation strategies aimed at reducing plastic pollution in the region. In this context, it is necessary to strengthen integrated solid waste management and urban discharge control in the Chili River basin in order to reduce the generation and input of microplastics (MPs) into the fluvial system. Considering that river water is used for agricultural irrigation, the presence of MPs may represent a potential pathway for transfer to soils, crops, and livestock, with possible implications for the food chain and regional food security. Thus, future research should prioritize evaluating the accumulation, environmental dynamics, and potential ecotoxicological effects of MPs in Andean agroecosystems.

Author Contributions: Conceptualization, Gerby Giovanna Rondán-Sanabria. Data curation, Gerby Giovanna Rondán-Sanabria and Italo Francisco Treviño-Zevallos. Formal analysis, Gerby Giovanna Rondán-Sanabria; Holger Saul Perez-Montaño. Funding acquisition, Gerby Giovanna Rondán-Sanabria. Investigation, Gerby Giovanna Rondán-Sanabria, Italo Francisco Treviño-Zevallos, Edgard Ronny Delgado Huamani. Methodology, Gerby Giovanna Rondán-Sanabria and Holger Saul Perez-Montaño. Project administration, Gerby Giovanna Rondán-Sanabria. Resources, Holger Saul Perez-Montaño. Software, Gerby Giovanna Rondán-Sanabria and Holger Saul Perez-Montaño. Supervision, Gerby Giovanna Rondán-

Sanabria. Validation, Holger Saul Perez-Montaña; Gerby Giovanna Rondán-Sanabria. Visualization, Gerby Giovanna Rondán-Sanabria. Writing – original draft, Gerby Giovanna Rondán-Sanabria. Writing – review and editing, Gerby Giovanna Rondán-Sanabria, Italo Francisco Treviño-Zevallos, Edgard Ronny Delgado Huamani and Holger Saul Perez-Montaña.

Funding: “This research was funded by the Universidad Tecnológica del Perú through the internal research project P - 2024-SUR-10.

Institutional Review Board Statement: “Not applicable.”

Informed Consent Statement: “Not applicable.” (for studies not involving humans)

Acknowledgments: The authors are sincerely grateful acknowledge the Universidad Tecnológica del Perú for providing financial support to carry out this project. The authors also thank the Le Qara Research Laboratory for their valuable technical assistance and support in the FTIR-ATR analyses, as well as for their collaboration and expertise throughout the analytical process.

Conflicts of Interest: “The authors declare that they have no conflicts of interest”

REFERENCES

1. Alam, M.J., Shammi, M. and Tareq, S.M., 2023. Distribution of microplastics in shoreline water and sediment of the Ganges River Basin to Meghna Estuary in Bangladesh. *Ecotoxicology and Environmental Safety*, 266(June), p. 115537. Available at: <https://doi.org/10.1016/j.ecoenv.2023.115537>.
2. Allen, N.S., Edge, M., Rodriguez, M., Liauw, C.M., Fontan, E., 2000. Aspects of the thermal oxidation of ethylene vinyl acetate copolymer. *Polymer Degradation and Stability*, 68(3), pp. 363–371. Available at: [https://doi.org/10.1016/S0141-3910\(00\)00020-3](https://doi.org/10.1016/S0141-3910(00)00020-3).
3. Anuar, S.T., Abdullah, N.S., Yahya, N.K.E.M., Chin, T.T., Yusof, K.M.K.K., Mohamad, Y., Azmi, A.A., Jaafar, M., Mohamad, N., Khalik, W.M.A.W.M., Ibrahim, Y.S., 2023. A multidimensional approach for microplastics monitoring in two major tropical river basins, Malaysia. *Environmental Research*, 227(March), p. 115717. Available at: <https://doi.org/10.1016/j.envres.2023.115717>.
4. Banda, A.A.P., Elguera, N.Y.M., Oviedo, A.A.P., Cueva, D.M.D., Semensatto, D., Brito, H.D., Zornio, B.F., Pacheco, H.G.J., 2025. Characteristics, abundance, distribution, and degradation dynamics of microplastics in the high Colca-Chilli water transfer systems: Tracing an emergent pollutant to Andean reservoirs. *Science of the Total Environment*, 1003(September). Available at: <https://doi.org/10.1016/j.scitotenv.2025.180632>.

5. Barnes, D.K.A., Galgani, F., Thompson, R.C., Barlaz, M., 2009. Accumulation and fragmentation of plastic debris in global environments. *Philosophical Transactions of the Royal Society B: Biological Sciences*, 364(1526), pp. 1985–1998. Available at: <https://doi.org/10.1098/rstb.2008.0205>.
6. Belli, I.M., Vieira, E.S., Oliveira, A.R., Pinto, L., Garbossa, L.H.P., Bayard, R., Franco, D., Dantas, D.V., de Castilhos Junior, A.B., 2026. Microplastics in Brazilian rivers: An overview and a study of floating particle accumulation on the coast of Santa Catarina state. *Science of the Total Environment*, 1012(August 2025). Available at: <https://doi.org/10.1016/j.scitotenv.2025.181224>.
7. Büngener, L., Schäffer, S.M., Schwarz, A., Schwalb, A., 2024. Microplastics in a small river: Occurrence and influencing factors along the river Oker. Northern Germany, *Journal of Contaminant Hydrology*, 264(January). Available at: <https://doi.org/10.1016/j.jconhyd.2024.104366>.
8. Carpio Fernández, J., Quispe, B., Fluquer, Y., Laureano, P., Sulca, P., Lima, O., 2022. Dirección de Geología Ambiental y Riesgo Geológico Equipo de Investigación: Hidrogeología de la cuenca del río Quilca-Vitor-Chili (132).
9. Chen, Z., Hay, J.N. and Jenkins, M.J., 2012. FTIR spectroscopic analysis of poly(ethylene terephthalate) on crystallization, *European Polymer Journal*, 48(9), pp. 1586–1610. Available at: <https://doi.org/10.1016/J.EUR-POLYMJ.2012.06.006>.
10. Chiu, H.T., Hsiao, Y.K., 2005. Compatibilization of Poly(ethylene terephthalate)/Polypropylene Blends with Maleic Anhydride Grafted Polyethylene-Octene Elastomer. *Journal of Polymer Research*, 13, pp. 153–160. Available at: <https://doi.org/10.1007/S10965-005-9020-Z>.
11. Coleman, M.M., Lee, K.H., Skrovanek, D.J., Painter, P.C., 2002. Hydrogen bonding in polymers. 4. Infrared temperature studies of a simple polyurethane. *Macromolecules*, 19(8), pp. 2149–2157. Available at: <https://doi.org/10.1021/MA00162A008>.
12. Demri, D., Hindermann, J.P., Diagne, C., Kiennemann, A., 1994. Formation of C2 oxygenates on rhodium-containing catalysts during CO + H₂ reactions. FTIR study of acetaldehyde adsorption. *Journal of the Chemical Society, Faraday Transactions*, 90(3), pp. 501–506. Available at: <https://doi.org/10.1039/FT9949000501>.
13. Deocarís, C.C., Fernández, M.C., Lee, A.R., Miao, S.L.A., Padolina, J.B.P., 2023. Identification and Characterization of Microplastics on the Surface Water in Laguna de Bay, Philippines. *Nature Environment and Pollution Technology*, 22(2), pp. 1073–1080. Available at: <https://doi.org/10.46488/NEPT.2023.v22i02.055>.
14. Dimassi, S.N., Hahladakis, J.N., Daly Yahia, M.N., Ahmad, M.I., Sayadi, S., Al-Ghouti, M.A., 2023. Insights into the degradation mechanism of PET and PP under marine conditions using FTIR. *Journal of Hazardous Materials*, 447, p. 130796. Available at: <https://doi.org/10.1016/J.JHAZMAT.2023.130796>.
15. Dodi, G., Popescu, D., Cojocaru, F.D., Aradoaei, M., Ciobanu, R.C., Mihai, C.T., 2022. Use of Fourier-Transform Infrared Spectroscopy for DNA Identification on Recycled PET Composite Substrate. *Applied Sciences*, Vol. 12, Page 4371, 12(9), p. 4371. Available at: <https://doi.org/10.3390/APP12094371>.

16. dos Santos Silva, J., Cidade, M.J.A., Panero, F. dos S., Ribeiro, L.B., Campos da Rocha, F.O., 2024. Microplastic pollution in the Amazon Basin: Current scenario, advances and perspectives. *Sci. Total Environ.* 946, 174150. <https://doi.org/10.1016/j.scitotenv.2024.174150>.
17. Fernández-González, V., Andrade-Garda, J.M., López-Mahía, P., Muniategui-Lorenzo, S., 2021. Impact of weathering on the chemical identification of microplastics from usual packaging polymers in the marine environment. *Analytica Chimica Acta*, 1142, pp. 179–188. Available at: <https://doi.org/10.1016/J.ACA.2020.11.002>.
18. Gewert, B., Plassmann, M.M., Macleod, M., 2015. Pathways for degradation of plastic polymers floating in the marine environment. *Environmental Science: Processes & Impacts*, 17(9), pp. 1513–1521. Available at: <https://doi.org/10.1039/C5EM00207A>.
19. Giarrizzo, T., Andrade, M.C., Schmid, K., Winemiller, K.O., Ferreira, M., Pegado, T., Chelazzi, D., Cincinelli, A., Fearnside, P.M., 2019. Amazonia: the new frontier for plastic pollution. *Frontiers in Ecology and the Environment*, 17(6), pp. 309–310. Available at: <https://doi.org/10.1002/fee.2071>.
20. Glaser, T.K., Plohl, O., Vesel, A., Ajdnik, U., Ulrih, N.P., Hrnčič, M.K., Bren, U., Zemljič, L.F., 2019. Functionalization of Polyethylene (PE) and Polypropylene (PP) Material Using Chitosan Nanoparticles with Incorporated Resveratrol as Potential Active Packaging. *Materials*, Vol. 12, Page 2118, 12(13), p. 2118. Available at: <https://doi.org/10.3390/MA12132118>.
21. Gune, R., Martin, A., 2025. Microplastics in our diet: A review of food source contamination. *Food Control*. Elsevier Ltd. Available at: <https://doi.org/10.1016/j.foodcont.2025.111486>.
22. Harini, R., Sandhya, K., Sunil, C.K., Natarajan, V., 2025. Seaweed as a sink for microplastic contamination: Uptake, identifications and food safety implications. *Environmental Research*. Academic Press Inc. Available at: <https://doi.org/10.1016/j.envres.2025.121631>.
23. He, H., Yu, T., Chen, X., Yang, Y., Li, F., Gan, H., 2025. Observation, distribution, and characteristics of microplastics in sediments from the estuary and river network areas of Pearl River Delta, China. *Regional Studies in Marine Science*, 81. Available at: <https://doi.org/10.1016/j.rsma.2024.103977>.
24. Hidalgo-Ruz, V., - Gutow, L., - Thompson, R.C., - Thiel, M., 2012. Microplastics in the Marine Environment: A Review of the Methods Used for Identification and Quantification. *Environmental Science & Technology*, 46(6), p.3060-3075. Available at: <https://doi.org/10.1021/es2031505>
25. Ioakeimidis, C., Fotopoulou, K.N., Karapanagioti, H.K., Geraga, M., Zeri, C., Papathanassiou, E., Galgani, F., Papatheodorou, & G., 2016. The degradation potential of PET bottles in the marine environment: An ATR-FTIR based approach. *Scientific reports*, 6, 23501. Available at: <https://doi.org/10.1038/srep23501>.
26. Islam, N., Akter, F., Hossen, M.Y., Bhuiyan, T., Siddique, M.A.M., 2025. Microplastic pollution in the Jamuna River, Bangladesh: Abundance, polymer types, characteristics, and sources in riverbank and riverbed sediments. *Journal of Hazardous Materials: Plastics*, 1, p. 100006. Available at: <https://doi.org/10.1016/j.hazmp.2025.100006>.

27. Jin, J., Chen, S., Zhang, J., 2010. UV aging behaviour of ethylene-vinyl acetate copolymers (EVA) with different vinyl acetate contents. *Polymer Degradation and Stability*, 95(5), pp. 725–732. Available at: <https://doi.org/10.1016/J.POLYMDEGRADSTAB.2010.02.020>.
28. Joshi, C., Phyllei, S.W.E., Bhatt, S., Chatterjee, S., 2025. Microplastic surge in the Ariyankuppam river, Puducherry, India: A study on abundance, characterization, and pollution load index. *Journal of Contaminant Hydrology*, 274. Available at: <https://doi.org/10.1016/j.jconhyd.2025.104669>.
29. Khan, A.B., Perea, O., Sparks, C., Opeolu, B., 2025a. Assessing microplastic characteristics and abundance in the sediment and surface water of the Diep River. *Environmental Pollution*, 381(May), p. 126555. Available at: <https://doi.org/10.1016/j.envpol.2025.126555>.
30. Khan, A.B., Perea, O., Sparks, C., Opeolu, B., 2025b. Assessing microplastic characteristics and abundance in the sediment and surface water of the Diep River, Western Cape, South Africa. *Environmental Pollution*, 381. Available at: <https://doi.org/10.1016/j.envpol.2025.126555>.
31. Khan, A.B., Perea, O., Sparks, C., Opeolu, B., 2025c. Assessing microplastic characteristics and abundance in the sediment and surface water of the Diep River, Western Cape, South Africa.. *Environmental Pollution*, 381, p. 126555. Available at: <https://doi.org/10.1016/J.ENVPOL.2025.126555>.
32. Kotov, N., Keskitalo, M.M., Johnson, C.M., 2025. Nano FTIR spectroscopy of liquid water in the –OH stretching region. *Spectrochim. Acta Part A: Molecular and Biomolecular Spectroscopy*, 330, p. 125640. Available at: <https://doi.org/10.1016/J.SAA.2024.125640>.
33. Kunz, A., Schneider, F., Anthony, N., Lin, H.T., 2023. Microplastics in rivers along an urban-rural gradient in an urban agglomeration: Correlation with land use, potential sources and pathways. *Environmental Pollution*, 321(January), p. 121096. Available at: <https://doi.org/10.1016/j.envpol.2023.121096>.
34. Larrea Valdivia, A.E. et al. (2025) “First evidence of microplastics in the Quilca-Vitor-Chili river basin, Arequipa Larrea Valdivia, A.E., Larico, J.R., Huilca, C.V., Arias, A.H., 2025. First evidence of microplastics in the Quilca-Vitor-Chili river basin, Arequipa region, Peru. *Journal of Contaminant Hydrology*, 269(November 2024). Available at: <https://doi.org/10.1016/j.jconhyd.2024.104484>.
35. Lau, W.W.Y., Shiran, Y., Bailey, R.M., Cook, E., Stuchtey, M.R., Koskella, J., Velis, C.A., Godfrey, L., Boucher, J., Murphy, M.B., Thompson, R.C., Jankowska, E., Castillo, A.C., Pilditch, T.D., Dixon, B., Koerselman, L., Kosior, E., Favoino, E., Gutberlet, J., Baulch, S., Atreya, M.E., Fischer, D., He, K.K., Petit, M.M., Sumaila, U.R., Neil, E., Bernhofen, M. V., Lawrence, K., Palardy, J.E., 2020. Evaluating scenarios toward zero plastic pollution. *Science*, 369(6509), pp. 1455–1461. Available at: <https://doi.org/10.1126/SCIENCE.ABA9475>.
36. Lebreton, L., Andrady, A., 2019. Future scenarios of global plastic waste generation and disposal. *Palgrave Communications*, 5(1), pp. 1–11. Available at: <https://doi.org/10.1057/s41599-018-0212-7>.

37. Liu, X., Zhou, W., Cheng, P., Zhang, F., Tan, L., Fu, Y., Fan, Y., Lan, J., Gu, H., Liu, W., Wang, T., 2025. Microplastics: an overlooked particle organic carbon in river systems. *Science Bulletin*, 70(21), pp. 3499–3503. Available at: <https://doi.org/10.1016/j.scib.2025.06.022>.
38. Ma, G., Li, K., Zou, W., Xin, R., Zhang, X., Feng, J., Chen, Z., Yang, Y., Lou, X., Zhang, K., Yang, F., 2025. Agricultural plastic Legacy in river Sediments: Abundance, oxidation, and occurrence characteristics of microplastics across rural China. *Environmental Pollution*, 385. Available at: <https://doi.org/10.1016/j.envpol.2025.127096>.
39. Maheswaran, B., Karmegam, N., Al-Ansari, M., Subbaiya, R., Al-Humaid, L., Sebastin Raj, J., Govarthan, M., 2022. Assessment, characterization, and quantification of microplastics from river sediments. *Chemosphere*, 298, p. 134268. Available at: <https://doi.org/10.1016/J.CHEMOSPHERE.2022.134268>.
40. Mahmud, F., Roy, H., Bhuiyan, M.M.K., Islam, M.S., 2025a. Critical analysis, characterization, and treatment of microplastics in the peripheral rivers of Dhaka city: Buriganga and Turag. *Environ. Environmental Science: Advances* [Preprint]. Available at: <https://doi.org/10.1039/d5va00118h>.
41. Mahmud, F., Roy, H., Bhuiyan, M.M.K., Islam, M.S., 2025b. Critical analysis, characterization, and treatment of microplastics in the peripheral rivers of Dhaka city: Buriganga and Turag. *Environmental Science: Advances*, pp. 1810–1833. Available at: <https://doi.org/10.1039/d5va00118h>.
42. Mishra, A.K., Chattopadhyay, D.K., Sreedhar, B., Raju, K.V.S.N., 2006. FT-IR and XPS studies of polyurethane-urea-imide coatings. *Progress in Organic Coatings*, 55(3), pp. 231–243. Available at: <https://doi.org/10.1016/J.PORGCOAT.2005.11.007>.
43. Oreski, G., Wallner, G.M., 2009. Evaluation of the aging behavior of ethylene copolymer films for solar applications under accelerated weathering conditions. *Solar Energy*, 83(7), pp. 1040–1047. Available at: <https://doi.org/10.1016/J.SOLENER.2009.01.009>.
44. Österlund, H., Blecken, G., Lange, K., Marsalek, J., Gopinath, K., Viklander, M., 2023. Microplastics in urban catchments: Review of sources, pathways, and entry into stormwater. *Science of the Total Environment*, 858(July 2022). Available at: <https://doi.org/10.1016/j.scitotenv.2022.159781>.
45. Peng, G., Xu, P., Zhu, B., Bai, M., Li, D., 2018. Microplastics in freshwater river sediments in Shanghai, China: A case study of risk assessment in mega-cities. *Environmental Pollution*, 234, pp. 448–456. Available at: <https://doi.org/10.1016/j.envpol.2017.11.034>.
46. Phan, S., Padilla-Gamiño, J.L., Luscombe, C.K., 2022. The effect of weathering environments on microplastic chemical identification with Raman and IR spectroscopy: Part I. polyethylene and polypropylene. *Polymer Testing*, 116. Available at: <https://doi.org/10.1016/J.POLYMERTESTING.2022.107752>.
47. Rozenberg, M., Loewenschuss, A. and Marcus, Y. (1998) “IR spectra and hydration of short-chain polyethyleneglycols,” *Spectrochimica Acta Part A: Molecular and Biomolecular Spectroscopy*, 54(12), pp. 1819–1826. Available at: [https://doi.org/10.1016/S1386-1425\(98\)00062-6](https://doi.org/10.1016/S1386-1425(98)00062-6).

48. Skrovanek, D.J., Painter, P.C., Coleman, M.M., 2002. Hydrogen bonding in polymers. 2. Infrared temperature studies of nylon 11. *Macromolecules*, 19(3), pp. 699–705. Available at: <https://doi.org/10.1021/MA00157A037>.
49. Tariq, A., Afzal, A., Rashid, I.A., Shakir, M.F., 2020. Study of thermal, morphological, barrier and viscoelastic properties of PP grafted with maleic anhydride (PP-g-MAH) and PET blends. *Journal of Polymer Research*, 27:10, 27(10), pp. 309-. Available at: <https://doi.org/10.1007/S10965-020-02291-2>.
50. Ullah, H., Hafeez, S., Mian, I.A., Khan, Aamir Ahsan, Khan, Aitezaz Ahsan, Khan, B., 2025. Seasonal microplastic pollution in surface water and sediments of the Swat and Kabul Rivers, Pakistan. *Journal of Environmental Chemical Engineering*, 13(3). Available at: <https://doi.org/10.1016/j.jece.2025.117048>.
51. Upadhyay, K., Bajpai, S., 2021. Microplastics in Landfills: A Comprehensive Review on Occurrence, Characteristics and Pathways to the Aquatic Environment. *Nature Environment and Pollution Technology*, 20(5), pp. 1935–1945. Available at: <https://doi.org/10.46488/NEPT.2021.V20I05.009>.
52. Valdés, B.S.G., Gomes, C.S.B., Gomes, P.T., Ascenso, J.R., Diogo, H.P., Gonçalves, L.M., dos Santos, R.G., Ribeiro, H.M., Bordado, J.C., 2018. Synthesis and Characterization of Isosorbide-Based Polyurethanes Exhibiting Low Cytotoxicity Towards HaCaT Human Skin Cells. *Polymers*, 10(10), p.1170. Available at: <https://doi.org/10.3390/POLYM10101170>.
53. Venkatachalam, S., Radhakrishnan, N., 2025. Assessment and quantification of microplastics in northern Tamil Nadu estuaries: Distributional dynamics and ecological threats from intertidal mangrove ecosystems. *Physics and Chemistry of the Earth*, 141. Available at: <https://doi.org/10.1016/j.pce.2025.104187>.
54. Wang, C.B., Cooper, S.L., 2002. Morphology and properties of segmented polyether polyurethaneureas. *Macromolecules*, 16(5), pp. 775–786. Available at: <https://doi.org/10.1021/MA00239A014>.
55. Xiang, X., Liu, Y., Tang, L., Xueying, L., Xinrong, S.U., 2026. Microplastic pollution in Chinese Rivers: A detailed analysis of distribution, risk factors, and ecological impact. *Marine Pollution Bulletin*, 222. Available at: <https://doi.org/10.1016/j.marpolbul.2025.118676>.
56. Xu, K., Shahab, A., Rinklebe, J., Xiao, H., Li, J., Ye, F., Li, Y., Wang, D., Bank, M.S., Wei, G., 2024. Spatial distribution, morphology, and risk assessment of microplastics in sediment from the Pearl River Estuary, China. *Emerging Contaminants*, 10(3), p. 100383. Available at: <https://doi.org/10.1016/J.EMCON.2024.100383>.
57. Yang, H., Sun, F., Liao, H., Huang, L., Zhao, Q., Wu, F., 2024. Pollution characterization and multi-index ecological risk assessment of microplastics in urban rivers from a Chinese megacity. *Journal of Hazardous Materials*, 480. Available at: <https://doi.org/10.1016/j.jhazmat.2024.136145>.
58. Yang, Z., Suzuki, T., Viyakarn, V., Hagita, R., Joshima, H., Arakawa, H., 2025. Pollution, degradation, and risk assessment of microplastic (> 30 µm) in subsurface (5 m) seawaters along Tokyo-Bangkok shipping route. *Science of the Total Environment*, 998. Available at: <https://doi.org/10.1016/j.scitotenv.2025.180261>.

-
59. De Zea Bermudez, V., Carlos, L.D., Alcácer, L., 1999. Sol–Gel Derived Urea Cross-Linked Organically Modified Silicates. 1. Room Temperature Mid-Infrared Spectra. *Chemistry of Materials*, 11(3), pp. 569–580. Available at: <https://doi.org/10.1021/CM980372V>.